Phase-Separated DCSK: A Simple Delay-Component-Free Solution for Chaotic Communications

Hua Yang, Guo-Ping Jiang, *Member, IEEE*, and Junyi Duan

***Abstract*—In this brief, a phase-separated differential chaos shift keying (PS-DCSK) modulation scheme is proposed as a simple delay-component-free version of DCSK modulation. Separated by orthogonal sinusoidal carriers rather than time delay, the reference and information-bearing signals in DCSK are transmitted simultaneously and parallel in the proposed system. As a result, PS-DCSK not only can avoid the difficult-to-implement radio-frequency delay line problem but also can achieve a doubled attainable data rate, enhanced communication security, and equivalent bit-error-rate (BER) performance with respect to DCSK. Finally, analytical expressions for the BER performance of the proposed system are derived and verified by computer simulation results over additive Gaussian white noise and Rayleigh fading channels.**

***Index Terms*—Bit error rate (BER), chaos communications, delay component, differential chaos shift keying (DCSK), phase-separated DCSK (PS-DCSK).**

I. Introduction

SINCE nonperiodic and easy-to-generate chaotic signals were applied to digital communication, chaotic modulation schemes have attracted considerable research interests and lots of communication systems based on chaos have been suggested and studied for different applications [1]–[10]. By utilizing the wideband chaotic segments with perfect correlation property, chaos-based communications demonstrate numerous attractive features, including low probability of detection, high data security, and resistance against multipath fading [11].

To avoid the chaotic synchronization problem, which is rather difficult to solve at the receiver side, most noncoherent chaotic communication systems (such as differential chaos shift keying (DCSK) in [2] and [3], frequency-modulated DCSK (FM-DCSK) in [4], permutation-based DCSK in [5], and enhanced versions of DCSK for increased data rate in [6]–[8]) employ the transmitted-reference (TR) technique in [12] to achieve good performance without channel estimation and chaotic synchronization. In these systems, the chaotic reference and information-bearing wavelets are sent separately in consecutive time slots. As a result, delay components inevitably become essential to both the transmitters and the receivers so that the previously mentioned two signals can be separated in the time domain.

Unfortunately, in ultrawideband (UWB) communications, radio-frequency (RF) delay lines are rather difficult to integrate in CMOS technology. To develop an alternative solution in which the need for delay components can be avoided in receivers, the code-shifted DCSK (CS-DCSK) scheme in [9] utilizes Walsh codes to distinguish the reference and information-bearing signals that are transmitted simultaneously. For a higher data rate, the high-data-rate CS-DCSK (HCS-DCSK) uses chaotic signals to substitute the Walsh codes in CS-DCSK [10].

Although all RF delay lines have been removed from the receivers in both CS-DCSK and HCS-DCSK systems, many more delay lines are introduced into their transmitters, making the system design more sophisticated and hardly integration friendly. Moreover, using Walsh codes or chaotic signals to separate the reference and information-bearing signals also brings CS-DCSK and HCS-DCSK systems additional synchronization requirements, i.e., Walsh code synchronization in a CS-DCSK system and chaotic signal synchronization in an HCS-DCSK system. In fact, these new synchronization requirements, particularly the one associated with HCS-DCSK, are quite difficult to satisfy at the receiver side, which will complicate their system design and eventually limit the applications of these two systems in many aspects.

To achieve simultaneous and parallel transmission of the reference and information-bearing wavelets with a low cost of implementation, a novel phase-separated DCSK (PS-DCSK) scheme is proposed in this brief. In our scheme, the reference and data-bearing signals are modulated separately onto in-phase and quadrature sinusoidal wavelets so that these two signals could be sent via orthogonal I and Q channels at the same time, respectively. In consequence, demands for delay lines and switches have been eliminated in both the transmitters and the receivers of PS-DCSK, making its system architecture free of delay components. Furthermore, without any performance loss, this new system can obtain doubled attainable bit transmission rate and enhanced data privacy (like method presented in [5], bit rate is also made undetectable from the frequency spectrum in the proposed scheme) in comparison with DCSK.

Manuscript received May 29, 2014; accepted September 3, 2014. Date of publication September 10, 2014; date of current version December 1, 2014. This work was supported in part by the National Natural Science Foundation of China under Grants 61374180 and 61401226, and in part by the Ministry of Education Research, Humanities and Social Sciences Planning Fund of China under Grant12YJAZH120. This brief was recommended by Associate Editor Y. Nishio.

H. Yang is with the School of Electronic Science and Engineering, Nanjing University of Posts and Telecommunications, Nanjing 210003, China (e-mail: yangh@njupt.edu.cn).

G.-P. Jiang is with the School of Automation, Nanjing University of Posts and Telecommunications, Nanjing 210003, China (e-mail: jianggp@njupt.edu.cn).

J. Duan is with the School of Communication and Information Engineering, Nanjing University of Posts and Telecommunications, Nanjing 210003, China (e-mail: duanjunyi922@126.com).

Color versions of one or more of the figures in this brief are available online at http://ieeexplore.ieee.org.

Digital Object Identifier 10.1109/TCSII.2014.2356914

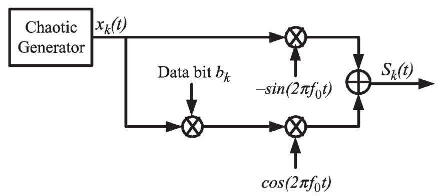

Fig. 1. Transmitter structure.

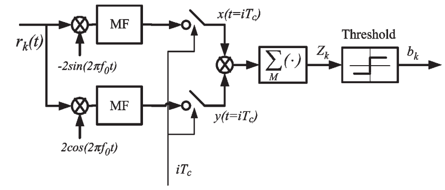

Fig. 2. Block diagram of the receiver.

II. Principle of PS-DCSK Scheme

Here, a novel simultaneous and parallel transmission method will be applied to DCSK, in which the separation of the reference and the information-bearing signals is performed by orthogonal sinusoidal carriers rather than the time delay in the original DCSK in [2]. Without loss of generality, the proposed method is also applicable to many other chaotic modulation schemes that use TR technique (such as FM-DCSK, correlation delay shift keying, and quadrature chaos shift keying), the details of which will be described elsewhere due to brief length limitation.

A possible PS-DCSK transmitter structure is given for simple implementation in Fig. 1, in which no delay lines are involved. In addition, as no switching is performed in Fig. 1, a continuous operation of the transmitter is allowed. For each data bit, the chaotic generator will first output certain chaotic wavelet as the reference, and then, the generated reference and its identical or inversed copy will be modulated onto quadrature and in-phase sinusoidal carriers, respectively. Finally, the reference and data-bearing signals will be transmitted at the same time via the I and Q channels independently for minimized interference.

If the transmission of a single isolated data bit b_k is considered, the reference signal generated by the chaotic generator is given as

$$x_k(t) = \sum_{i=(k-1)M}^{kM-1} x_i h_T(t - iT_c), (k-1)MT_c \leq t < kMT_c \tag{1}$$

where x_i denotes the chaotic sample generated by the logistic map $x_{i+1} = 1 - 2x_i^2$ in [13]. Here, T_c is the chip duration, and M is the length of the chaotic spreading sequence. $h_T(t)$ is the pulse signal with duration of T_c, the shape of which could be rectangular, raised cosine, or other ones. In this brief, $h_T(t)$ is defined as the impulse response of the square-root-raised-cosine filter, which has been normalized to have unit energy

$$\int_{iT_c}^{(i+1)T_c} h_T^2(t - iT_c)\, dt = 1, \quad i = 1, 2, 3, \ldots \tag{2}$$

Therefore, the transmitted signal in PS-DCSK system can be described as

$$S_k(t) = b_k x_k(t) \cos(2\pi f_0 t) - x_k(t) \sin(2\pi f_0 t), \quad (k-1)MT_c \leq t < kMT_c. \tag{3}$$

Here, the frequency of the sinusoidal carrier is f_0, which is assumed not only to be a multiple of $1/T_c$ but also to satisfy $f_0 \gg 1/T_c$.

Fig. 2 shows an available design of PS-DCSK receiver, where the received signal is first multiplied with the synchronized in-phase and quadrature carriers, respectively. The resulting signals are then fed into two identical matched filters (MFs) separately. Here, MFs, rather than low-pass filters, are utilized to maximize the output peak pulse signal-to-noise ratio at each sample time $t = iT_c$. Both of these two filters are designed to be matched to the pulse signal $h_T(t)$. Finally, the output of both MFs are sampled every iT_c time and the two obtained discrete sequences are correlated over the spreading sequence length M.

With assumptions that the received signal is only corrupted by additive Gaussian white noise (AWGN), the received signal is given as

$$r_k(t) = S_k(t) + n(t). \tag{4}$$

In which, $n(t)$ is a zero-mean stationary Gaussian noise with power spectral density of $N_0/2$.

If perfect carrier and bit synchronizations have been achieved, the outputs of the two samplers in Fig. 2 can be easily obtained by using the analysis method given in [14]

$$x(t = iT_c) = x_i + n_i^Q, \quad (k-1)M \leq i < kM \tag{5}$$
$$y(t = iT_c) = b_k x_i + n_i^I, \quad (k-1)M \leq i < kM \tag{6}$$

where n_i^I and n_i^Q are independent Gaussian random variables with mean values and variances given as

$$E\left[n_i^Q\right] = E\left[n_i^I\right] = 0 \tag{7}$$
$$\mathrm{var}\left[n_i^Q\right] = \mathrm{var}\left[n_i^I\right] = N_0. \tag{8}$$

Here, $E[\cdot]$ represents the expectation operator, and $\mathrm{var}[\cdot]$ represents the variance operator.

Consequently, the correlator output Z_k for data bit b_k is given by

$$Z_k = \sum_{i=(k-1)M}^{kM-1} \left(x_i + n_i^Q\right) \cdot \left(b_k x_i + n_i^I\right). \tag{9}$$

According to the following rules, the binary information bit could be easily retrieved, i.e.,

$$\hat{b}_k = \begin{cases} +1, & \text{if } Z_k > 0 \\ -1, & \text{if } Z_k \leq 0. \end{cases} \tag{10}$$

Compared with the original DCSK receiver in [2], merely a few circuits for in-phase and quadrature demodulations have been introduced into the receiver in Fig. 2, making our receiver only slightly complicated and also deserve a label of "simple." In addition, if the synchronization problem is concerned, only carrier and bit synchronization are involved in our receiver. To achieve perfect bit synchronization, lots of traditional timing techniques could be adopted here, such as inserting a synchronizing preamble as periodic reference. As for carrier synchronization, since the carrier recovery process in our scheme is almost identical to that in QPSK modulation, lots of techniques and circuits designed for carrier recovery in traditional telecommunication systems could be directly used in our system. For instance, the carrier-phase estimation circuit that is composed of a squared-law device, bandpass filter tuned to $2f_0$ and a phase-locked loop in [15] would be a nice choice. Therefore, the complexity cost of synchronization design has been greatly decreased in PS-DCSK, as the carrier synchronization in our scheme is actually much easier to acquire in comparison with the Walsh code synchronization in CS-DCSK and the chaos synchronization in HCS-DCSK.

III. Performance Analysis

Here, the bit-error-rate (BER) performance of the proposed system is analyzed over AWGN and Rayleigh fading channels, respectively. Since the Gaussian approximation method fails to be valid in case of small spreading sequence lengths, numerical integration (NI) method in [16] and [17] has been adopted here to improve the accuracy of the theoretical results.

A. AWGN Channel

To analyze the BER performance of the PS-DCSK system with an NI approach, the bit-error probability has to be evaluated first for a given transmitted bit energy. According to (3), the transmitted signal energy for a given data bit b_k can be computed as

$$\begin{aligned} E_b^{(k)} &= \int_{(k-1)MT_c}^{kMT_c} S_k^2(t)\,dt \\ &= \int_{(k-1)MT_c}^{kMT_c} x_k^2(t)\,dt - b_k \int_{(k-1)MT_c}^{kMT_c} x_k^2(t)\sin(4\pi f_0 t)\,dt \\ &= \sum_{i=(k-1)M}^{kM-1} x_i^2 \int_{iT_c}^{(i+1)T_c} h_T^2(t-iT_c)\,dt \\ &= \sum_{i=(k-1)M}^{kM-1} x_i^2. \end{aligned} \tag{11}$$

Considering $E_b^{(k)}$ in (11) as a deterministic variable, the decision variable in (9) can be regarded as a Gaussian random variable [18]. Thus, its distribution can be fully characterized by computing the conditional mean value and variance.

After simplification, (9) can be transformed as

$$\begin{aligned} Z_k = b_k \sum_{i=(k-1)M}^{kM-1} x_i^2 + \sum_{i=(k-1)M}^{kM-1} x_i n_i^I \\ + b_k \sum_{i=(k-1)M}^{kM-1} x_i n_i^Q + \sum_{i=(k-1)M}^{kM-1} n_i^I n_i^Q. \end{aligned} \tag{12}$$

Since the mean values of the latter three terms in (12) all equal to zero, it is readily to shown that the conditional mean value of decision variable Z_k is

$$E\left[Z_k | E_b^{(k)}\right] = b_k E_b^{(k)}. \tag{13}$$

Based on the statistical characteristics of x_i given in [13], it can be proved that the cross correlations between the four sum terms in Z_k are zero. Therefore, the conditional variance of Z_k could be easily derived as

$$\operatorname{var}\left[Z_k | E_b^{(k)}\right] = 2E_b^{(k)} N_0 + M N_0^2. \tag{14}$$

If b_k is assumed to be equiprobable, the bit-error probability of PS-DCSK system for a given $E_b^{(k)}$ can be computed as

$$\begin{aligned} P_e\left(E_b^{(k)}\right) &= \frac{1}{2}\operatorname{erfc}\left(\frac{\left|E\left[Z_k|E_b^{(k)}\right]\right|}{\sqrt{2\operatorname{var}\left[Z_k|E_b^{(k)}\right]}}\right) \\ &= \frac{1}{2}\operatorname{erfc}\left(\sqrt{\frac{E_b^{(k)}}{4N_0}\left(1+\frac{M}{2}\frac{N_0}{E_b^{(k)}}\right)^{-1}}\right). \end{aligned} \tag{15}$$

where $\operatorname{erfc}(\cdot)$ denotes the complementary error function [19].

By integrating the constant-bit-energy-assumption formula in (15) over the bit-energy distribution, the overall analytical BER expression of PS-DCSK system can be obtained as

$$\begin{aligned} &\mathrm{BER}_{\mathrm{AWGN}} \\ &= \int \frac{1}{2}\operatorname{erfc}\left(\sqrt{\frac{E_b^{(k)}}{4N_0}\left(1+\frac{M}{2}\frac{N_0}{E_b^{(k)}}\right)^{-1}}\right)\cdot p\left(E_b^{(k)}\right) dE_b^{(k)}. \end{aligned} \tag{16}$$

Here, $p(E_b^{(k)})$ is the probability density function (PDF) of the transmitted bit energy $E_b^{(k)}$. Interestingly, the BER expression in (16) is actually identical to that of DCSK system in [16].

B. Rayleigh Fading Channel

For easy of analysis, a simple slow fading channel model is adopted here and the received signal can be denoted by

$$r_k(t) = \lambda(t) S_k(t) + n(t) \tag{17}$$

in which $\lambda(t)$ is the channel coefficient that has the following Rayleigh PDF:

$$f_\lambda(y) = \frac{y}{\sigma^2} e^{-\frac{y^2}{2\sigma^2}}. \tag{18}$$

As the channel is slow fading, the channel coefficients are assumed to be constant during one bit duration and change to different independent values from one bit to another. Therefore, the decision variable for decoding bit b_k can be rewritten as

$$\begin{aligned} Z'_k = b_k \lambda_k^2 \sum_{i=(k-1)M}^{kM-1} x_i^2 + \lambda_k \sum_{i=(k-1)M}^{kM-1} x_i n_i^I \\ + \lambda_k b_k \sum_{i=(k-1)M}^{kM-1} x_i n_i^Q + \sum_{i=(k-1)M}^{kM-1} n_i^I n_i^Q. \end{aligned} \tag{19}$$

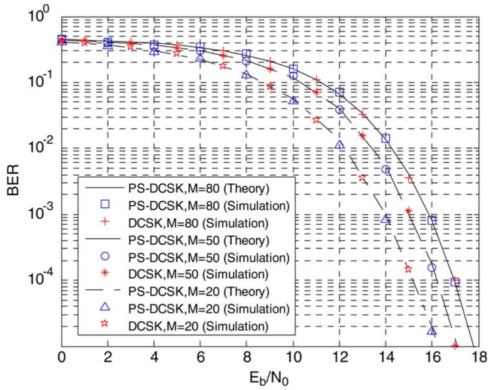

Fig. 3. Comparison of the simulation results and the theoretical estimates over an AWGN channel.

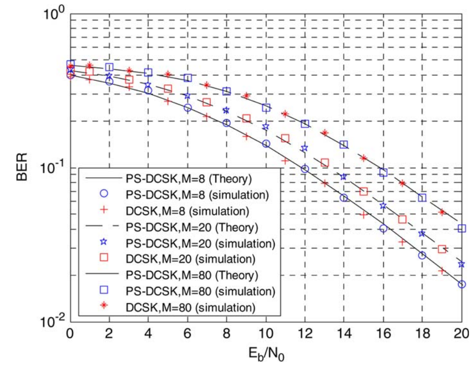

Fig. 4. BER performance of PS-DCSK and DCSK systems over a Rayleigh fading channel with average gain power $E[\lambda^2 = 0.9]$.

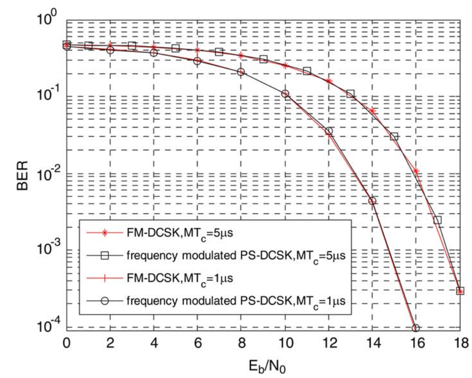

Fig. 5. Performance comparison of FM-DCSK and frequency-modulated PS-DCSK systems over AWGN channel.

For a given bit energy $E_b^{(k)}$ and channel coefficient λ_k, the decision variable Z_k' in (19) is necessarily a Gaussian random variable, whose mean value and variance under same conditions are listed as

$$E\left[Z_k'|E_b^{(k)},\lambda_k\right] = b_k\lambda_k^2 E_b^{(k)} \tag{20}$$

$$\mathrm{var}\left[Z_k'|E_b^{(k)},\lambda_k\right] = 2\lambda_k^2 E_b^{(k)} N_0 + MN_0^2. \tag{21}$$

Finally, the overall BER performance of PS-DCSK system over Rayleigh fading channel is

$$\mathrm{BER}_{\mathrm{Rayleigh}} = \iint \frac{1}{2}\mathrm{erfc}\left(\sqrt{\frac{E_b^{(k)}}{4N_0}\left(\frac{1}{\lambda_k^2}+\frac{M}{2\lambda_k^4}\frac{N_0}{E_b^{(k)}}\right)^{-1}}\right) \times p\left(E_b^{(k)}\right)p(\lambda_k)dE_b^{(k)}d\lambda_k \tag{22}$$

where $p(\lambda_k)$ is the PDF of channel coefficient λ_k.

If γ_b is used to denote the product $\lambda_k^2(E_b^{(k)}/N_0)$ in (22), expression (22) can be further simplified and rewritten as

$$\mathrm{BER}_{\mathrm{Rayleigh}} = \int \frac{1}{2}\mathrm{erfc}\left(\left[\frac{4}{\gamma_b}+\frac{2M}{\gamma_b^2}\right]^{-\frac{1}{2}}\right)p(\gamma_b)d\gamma_b \tag{23}$$

in which $p(\gamma_b)$ is the PDF of γ_b.

IV. Simulation Results

Here, PS-DCSK, DCSK, FM-DCSK, CS-DCSK, and HCS-DCSK systems are simulated over different channels (including AWGN and Rayleigh fading channels) at various E_b/N_0 levels. For comparison, relevant theoretical results are also computed by using the rectangular integration method, in which the entire integration interval is divided into 100 equal subintervals.

In Fig. 3, the simulated BER curves of PS-DCSK system under AWGN channel are compared with the analytical ones computed by (16). For comparison, Monte Carlo simulations of DCSK system over the AWGN channel are also plotted. Obviously, the simulated curves of PS-DCSK system match the theoretical ones quite well not only for large spreading sequence lengths but also for small spreading sequence lengths, which help to prove the validity of (16). In addition, it can also be found in Fig. 3 that the BER performance of the proposed system is equivalent to that of the DCSK system under the AWGN channel, which also matches the theoretical analysis in Section III.

In Fig. 4, the analytical results computed by (22) are shown with the simulated results of PS-DCSK system over the Rayleigh fading channel. Here, relevant Monte Carlo simulations of the DCSK system under Rayleigh fading channel are also plotted for comparison. Apparently, simulation results perfectly agree with our analytical ones for all spreading sequence lengths. In addition, the BER performances of DCSK and PS-DCSK systems over the Rayleigh fading channel appear to be identical too.

Simulated BER performances of FM-DCSK system and the frequency-modulated PS-DCSK system over AWGN channel are compared in Fig. 5. In our simulation, the center frequency of the FM modulator is 36 MHz, the gain of the FM modulator is 7.8 MHz/V, the bandwidth of the channel selection filter is 17 MHz, and the chip rate is 20 MHz. It can be discovered in Fig. 5 that the frequency-modulated PS-DCSK system shares the same BER performance with FM-DCSK system if identical system parameters are used.

Fig. 6 displays the simulation results for the second type of HCS-DCSK system (denoted as HCS-DCSK2 here), PS-DCSK and CS-DCSK systems under AWGN channel. In our simulation, the Walsh code sequence length in CS-DCSK system is set to 4, the number of bits transmitted in each symbol in HCS-DCSK2 is set to 1, and the length of chaotic spreading sequence in all systems is set to 32 and 128, respectively. In Fig. 6, performances of these three systems become worse when M increases, which can be attributed to the increasing negative contribution from the noise components (including the

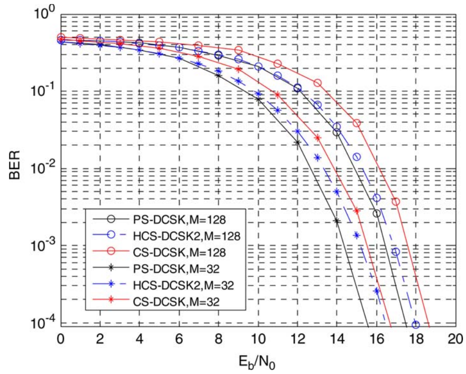

Fig. 6. Performance comparison between PS-DCSK, CS-DCSK, and HCS-DCSK2 systems with different lengths of chaotic spreading sequences under an AWGN channel.

noise-signal cross terms and noise–noise cross terms) in their own correlator outputs. In addition, it can also be observed in this same figure that the BER performance of PS-DCSK system appears to be better than that of CS-DCSK system, which is actually the result of reduced noise components in the correlator output of PS-DCSK. Moreover, it is also very interesting to find that our system performs slightly better than HCS-DCSK2 system in Fig. 6, and this performance gain over HCS-DCSK2 system seems more and more evident as M shrinks. This can be explained by the fact that HCS-DCSK2 system uses chaotic sequences to separate the reference and information-bearing signals, which will increase the uncertainty of the useful signal component in every correlator output, particularly in the case of small spreading sequence lengths.

V. Conclusion

A novel PS-DCSK modulation scheme has been developed and analyzed in this brief. Different from the conventional DCSK scheme that utilizes time delay to separate the reference and the data, the chaotic reference and data-carrying signals are, respectively, modulated onto two orthogonal sinusoidal carriers in the proposed system so that they could be simultaneously sent at the transmitter side and easily distinguished at receiver side. The analytical expressions for the BER performance of PS-DCSK in monouser case have been derived under AWGN and Rayleigh fading channels. Relevant computer simulation results are also given to prove the validity of our theoretical analysis.

With the help of this new signal separation method, the PS-DCSK system not only obtains doubled bit rate and enhanced data security in comparison with DCSK system but also has removed all delay components that might be difficult to implement in UWB communications from the transceivers. Furthermore, by comparing the BER performance of this novel scheme with that of DCSK scheme, it is proved that PS-DCSK and DCSK systems show equivalent BER performance in both AWGN and Rayleigh fading channels. These benefits will make the proposed scheme more attractive and more competitive in situations where CMOS technology is used for system implementation in UWB communications.

Compared with other chaotic modulation schemes designed for removing RF delay lines at the receiver side (including CS-DCSK and HCS-DCSK), the proposed scheme turns out to be a much simpler and cheaper solution to the simultaneous and parallel transmission of the reference and data. In contrast to CS-DCSK and HCS-DCSK systems, the proposed system dramatically simplifies the synchronization design and eventually greatly decreases the complexity cost of system implementation, since the demanding code/chaos synchronization has been replaced by carrier synchronization that is relatively easy to acquire.

Due to brief length limitation, the noise performance analysis of PS-DCSK modulation scheme over multipath fading channels or in multiuser applications will not be included in this brief and will be discussed in our future work.

Acknowledgment

The authors would like to thank Prof. G. Kaddoum of University of Québec, QC, Canada for the helpful discussions with him.

References

[1] H. Dedieu, M. P. Kennedy, and M. Hasler, "Chaos shift keying: Modulation and demodulation of a chaotic carrier using self-synchronizing Chua's circuit," *IEEE Trans. Circuits Syst. II, Analog Digit. Signal Process.*, vol. 40, no. 10, pp. 634–642, Oct. 1993.

[2] G. Kolumbán, B. Vizvki, W. Schwarz, and A. Abel, "Differential chaos shift keying: A robust coding for chaotic communication," in *Proc. NDES*, Seville, Spain, 1996, pp. 87–92.

[3] M. Suschik, L. S. Tsimring, and A. R. Volkovskii, "Performance analysis of correlation-based communication schemes utilizing chaos," *IEEE Trans. Circuits Syst. I, Fundam. Theory Appl.*, vol. 47, no. 12, pp. 1684–1691, Dec. 2000.

[4] G. Kolumbán, G. Kis, M. P. Kennedy, and Z. Jáko, "FM-DCSK: A new and robust solution to chaos communications," in *Proc. Int. Symp. Nonlinear Theory Appl.*, Hawaiian Village, HI, USA, 1997, pp. 117–120.

[5] F. C. M. Lau, K. Y. Cheong, and C. K. Tse, "Permutation-based DCSK and multiple access DCSK systems," *IEEE Trans. Circuits Syst. I, Fundam. Theory Appl.*, vol. 50, no. 6, pp. 733–742, Jun. 2003.

[6] Z. Galias and G. M. Maggio, "Quadrature chaos-shift keying: Theory and performance analysis," *IEEE Trans. Circuits Syst. I, Fundam. Theory Appl.*, vol. 48, no. 12, pp. 1510–1519, Dec. 2001.

[7] H. Yang and G.-P. Jiang, "High efficiency differential chaos shift keying scheme for chaos-based noncoherent communication," *IEEE Trans. Circuits Syst. II, Exp. Briefs*, vol. 59, no. 5, pp. 312–316, May 2012.

[8] H. Yang and G.-P. Jiang, "Reference-modulated DCSK: A novel chaotic communication scheme," *IEEE Trans. Circuits Syst. II, Exp. Briefs*, vol. 60, no. 4, pp. 232–236, Apr. 2013.

[9] W. K. Xu and L. Wang, "A novel differential chaos shift keying modulation scheme," *Int. J. Bifurcation Chaos*, vol. 21, no. 3, pp. 799–814, Mar. 2011.

[10] G. Kaddoum and F. Gagnon, "Design of a high-data-rate differential chaos-shift keying system," *IEEE Trans. Circuits Syst. II, Exp. Briefs*, vol. 59, no. 7, pp. 448–452, Jul. 2012.

[11] G. Kolumbán, M. P. Kennedy, and L. O. Chua, "The role of synchronization in digital communications using chaos—Part I: Fundamentals of digital communications," *IEEE Trans. Circuits Syst. I, Fundam. Theory Appl.*, vol. 44, no. 10, pp. 927–936, Oct. 1997.

[12] C. Rushforth, "Transmitted-reference techniques for random or unknown channels," *IEEE Trans. Inf. Theory*, vol. IT-10, no. 1, pp. 39–42, Jan. 1964.

[13] F. C. M. Lau and C. K. Tse, *Chaos-Based Digital Communication Systems*. Berlin, Germany: Springer-Verlag, 2003.

[14] S. Haykin, *Communication Systems*. Hoboken, NJ, USA: Wiley, 1994.

[15] J. G. Proakis, M. Salehi, and N. Zhou, *Communication Systems Engineering*. Upper Saddle River, NJ, USA: Prentice-Hall, 1994.

[16] G. Kaddoum, P. Charge, and D. Roviras, "A generalized methodology for bit-error-rate prediction in correlation-based communication schemes using chaos," *IEEE Commun. Lett.*, vol. 13, no. 8, pp. 567–569, Aug. 2009.

[17] G. Kaddoum, F. Richardson, and F. Gagnon, "Design and analysis of a multi-carrier differential chaos shift keying communication system," *IEEE Trans. Commun.*, vol. 61, no. 8, pp. 3281–3291, Aug. 2013.

[18] N. I. Chernov, "Limit theorems and Markov approximations for chaotic dynamical systems," *Probab. Theory Relat. Fields*, vol. 101, no. 3, pp. 321–362, 1995.

[19] J. G. Proakis, *Digital Communications*. New York, NY, USA: McGraw-Hill, 2001.